



Transient unsaturated flow in the drainage layer of a highway: solution and drainage performance

Han-Cheng Dan, Zhi Zhang, Xiang Liu & Jia-Qi Chen

To cite this article: Han-Cheng Dan, Zhi Zhang, Xiang Liu & Jia-Qi Chen (2019) Transient unsaturated flow in the drainage layer of a highway: solution and drainage performance, Road Materials and Pavement Design, 20:3, 528-553, DOI: [10.1080/14680629.2017.1397049](https://doi.org/10.1080/14680629.2017.1397049)

To link to this article: <https://doi.org/10.1080/14680629.2017.1397049>



Published online: 09 Nov 2017.



Submit your article to this journal [↗](#)



Article views: 128





View Crossmark data [↗](#)



Citing articles: 1 View citing articles [↗](#)



Transient unsaturated flow in the drainage layer of a highway: solution and drainage performance

Han-Cheng Dan ^a, Zhi Zhang^a, Xiang Liu ^{b*} and Jia-Qi Chen^{a,c}

^aSchool of Civil Engineering, Central South University, Changsha, People's Republic of China; ^bKey Laboratory of Traffic Safety on Track, Ministry of Education, School of Traffic & Transportation Engineering, Central South University, Changsha, People's Republic of China; ^cCenter for Advanced Infrastructure and Transportation, Rutgers, the State University of New Jersey, Piscataway, NJ, USA

(Received 6 April 2017; accepted 13 October 2017)

In order to quickly remove water entering pavement layers so as to mitigate water-induced damage, drainage layers are widely used in highway pavements. This paper introduces a 1-D mathematical model in order to quantify the transient behaviour of the groundwater flow in the drainage layer of highway pavements. The model takes into account the capillary effect and the nonlinear relationship between hydraulic conductivity and saturation. The analytical solution is obtained and validated against the 2-D Richards equation-based model. Then, sensitivity analysis is carried out and the results show that the drainage time is reduced and drainage efficiency is enhanced by capillarity. The drainage capacity (the total water drained from the drainage layer) depends on the water retention curve (e.g. α_G in the Gardner equation). In view of material selection, a relatively low value of α_G helps improve the drainage capacity of the drainage layer, whereas a suitable amount of fine particles also leads to a better drainage performance. Furthermore, the drainage material with hydraulic properties is recommended in terms of drainage performance improvement and strength requirement. The analytical solution, which is simple and easy to use, provides guidance for assessing the capillary effects on the effectiveness and efficiency of subsurface drainage systems of a highway.

Keywords: subsurface drainage systems; drainage layer; unsaturated flow; transient flow; Boussinesq equation

Notations

The following symbols are used in this paper:

D	length of the drainage layer [L]
H	water table elevation [L]
$\bar{H}(t)$	the average water table and it is a function of t only [L]
K	unsaturated hydraulic conductivity [LT^{-1}]
K_S	saturated hydraulic conductivity [LT^{-1}]
K_R	relative hydraulic conductivity
N	degree of nonlinear relationship between hydraulic conductivity and saturation [LT^{-1}]
S_e	effective saturation [–]
T	thickness of the drainage layer [L]

*Corresponding author. Email: xiangliu06@gmail.com

V	water volume in the drainage layer [L^3/L]
V_i	initial water volume in the drainage layer [L^3/L]
V_{t_D}	water volume at t_D in the drainage layer [L^3/L]
W_D	drainage ratio in the drainage layer [–]
x	horizontal coordinate [L]
x_1	the intersection point for the bottom of the drainage layer and calculated water table height
z	elevation [L]
α	slope angle [–]
α_G	the inverse of the mean capillary length (parameter of pore-size distribution) [L^{-1}]
β_G	a parameter accounting for the nonlinear relationship between the saturation and unsaturated hydraulic conductivity [L^{-1}]
θ	water content [–]
ϕ	effective porosity [–]
ψ	suction/capillary pressure head [L]
η	local groundwater depth [L]
$\bar{\eta}$	average groundwater depth [L]
λ	a parameter for representing the hydraulically related property of the drainage layer [L^2T]

1. Introduction

Practice has shown that asphaltic wearing surfaces which are exposed to water generally start losing aggregates prematurely through a damage phenomenon. This phenomenon has become known as asphaltic “stripping” or “raveling”, which is also called water-induced damage (Dan, He, Zhao, & Chen, 2015; Dawson, 2008). In general, specified open-graded mixtures are deliberately designed and laid to help drain pavement surface leaking water. The importance of providing adequate drainage in pavements has been demonstrated by previous researchers (e.g. Cedergren, 1974; Dawson, 2008). A rather common subsurface drainage system used to remove the infiltrated/seepage water from the pavement structures is by providing a drainage layer, in order to quickly remove water entering the pavement layers before any damage to the road can be initiated (Dawson, 2008). The water leaks from the pavement largely through cracks and joints and other unsealed openings in the surface (AASHTO, 1993; Cedergren, 1974; FHWA, 1992; Mallela, Titus-Glover, & Darter, 2000). In addition, when the drainage layer serves as a base or sub-base layer, its material must satisfy the requirements of both strength and permeability of a drainage layer (Ministry of Transport of the People’s Republic of China [MOTPRC], 2006; Dawson, 2008).

To date, pavement drainage systems have been frequently used in many countries, for example, China, Europe and the USA (Rabab’an, 2007). In a drained section, a drainage layer connected to a blind ditch (Figure 1(a)) (a trench covered with gravel or rock or containing a perforated pipe that redirects surface and groundwater away from the highway area (MOTPRC, 2012)) is often embedded under the pavement with the purpose of reducing water-induced damage (Al-Qadi, Lahouar, Louizi, Elseifi, & Wilkes, 2004; Dawson, 2008). At present, “time-to-drain” and “depth-of-flow” are the two basic concepts for designing a drainage layer. The first approach (time-to-drain) for designing the drainage layer, which was advocated by Casagrande and Shannon (1952), is to select a specific time to obtain a specified extent of drainage for an initially saturated drainage layer. Solutions for time-to-drain conditions were presented by both Casagrande and Shannon (1952) and Barber and Sawyer (1952). This method (AASHTO, 1993) assumed

that (1) water infiltrates into the pavement until the permeable base is saturated; (2) excess runoff will not enter the pavement section after it is saturated; and (3) after the rainfall event ceases, water is drained out through the blind ditch (Figure 1(a)). The second approach (depth-of-flow) is that the drainage layer should have steady flow efficiency not lower than the inflow from the surface. The water table in a drainage layer has been used as an indicator for the effectiveness of the drainage layer (i.e. a relatively low water table reflects an effective drainage design) (Moulton, 1979). Nowadays, most of the models used for designing a drainage layer are based on saturated flow. Dan, Xin, Li, Li, and Lockington (2012a) established a model (modifying the traditional Boussinesq equation with capillarity correction) to predict the water table at steady state in a drainage layer based on the design concept of depth-of-flow. This method aims to determine the minimum thickness required in designing a drainage layer. Since Dan et al.'s research (2012a) did not take transient flow into consideration, it is insufficient to quantify the drainage performance of a drainage layer. Based on Moulton (1979) and Dan's (2012a) work, Dan, Xin, Li, and Li (2013) established a model integrating the unsaturated flow in a drainage layer and that takes the transient flow into account based on the 1-D Boussinesq equation with capillary correction (water in the unsaturated zone). However, on the one hand, the solution derivation is somehow oversimplified to lead to deviation; thus it cannot degenerate to the saturated case; on the other hand, the relationship between the hydraulic conductivity and saturation is not taken into account. Furthermore, the factors that affect the drainage design still remain unclear.

Based upon Dan's earlier model (2013), this paper provides an improved model and conducts sensitivity analysis to guide and optimise the design of drainage layers. The paper is organised as follows: in Section 2, we incorporated the capillary effects into the transient Boussinesq equation-based model with the assumption of hydrostatic pressure distribution, and the solutions of water table and water storage are presented. In Section 3, the analytical solutions were validated against the predictions of a Richards equation-based model using the finite element method. In Section 4, sensitivity analysis was conducted in terms of the time taken to drain a specified quantity of water taking into consideration the drainage material and drainage geometric parameters, and the conclusions were drawn in Section 5.

2. Methodology

2.1. The model and the governing equation

Generally, the configuration of a drainage system is often uniform along the road direction and thus the system can be reduced to a two-dimensional model. Therefore, the recent research on a drainage system is largely focused on a two-dimensional cross-section as shown in Figure 1(a). Since Dan et al.'s previous work (Dan et al., 2012a; Dan, Xin, Li, Li, & Lockington, 2012b) revealed that the horizontal flow is dominant in the drainage layer, the 1-D Boussinesq equation neglecting the vertical flow can be employed to evaluate the flow in the drainage layer.

Based on the concept of "time-to-drain", the drainage layer is initially in a fully saturated state. As the drainage begins from the initial condition, the water table will gradually fall down to some extent. During the main drainage period of the drainage layer, the vadose zone can be divided into unsaturated and saturated zones as shown in Figure 1(b). According to the development of the water table height, the drainage process in the drainage layer can be classified as three conditions, namely, the initial completely saturated condition, early drainage condition and later drainage condition (Figure 1(b)). The water volume in the first condition is given as an initial condition and the flows in the second and third conditions need to be investigated accordingly. It is noted in advance that the water table in the third condition is partly below the bottom of the drainage layer (intersection point between the water table and the drainage layer bottom which

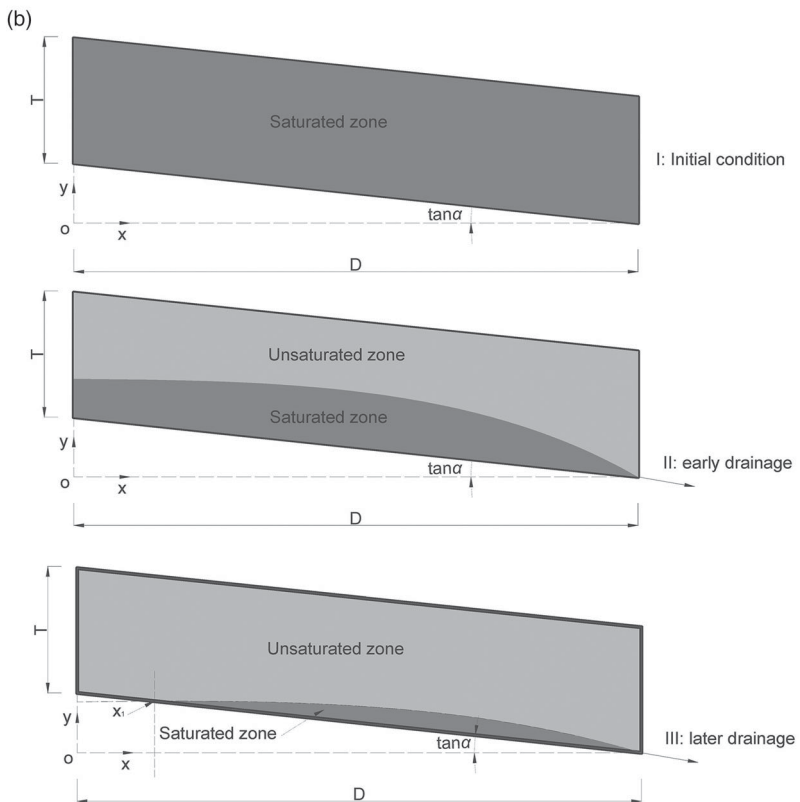
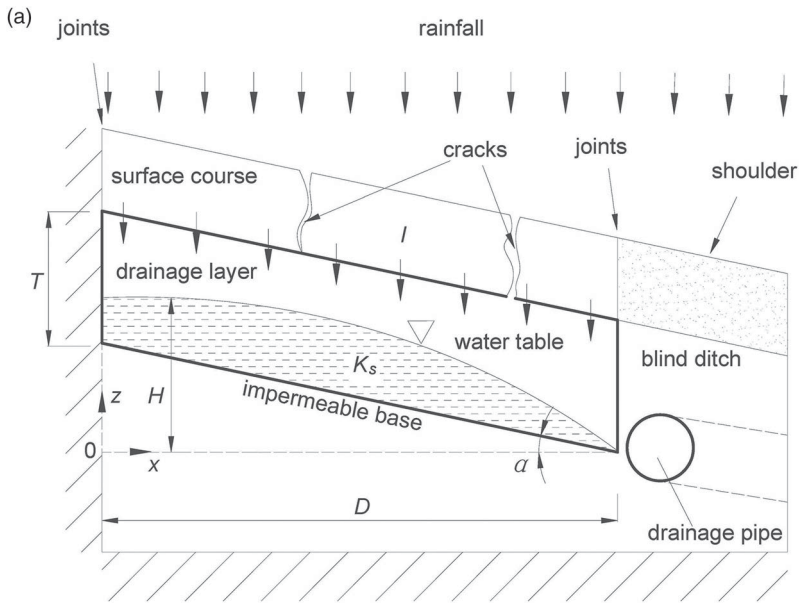


Figure 1. (a) Schematic diagram of a drainage system with the drainage layer of a highway pavement (Dan et al., 2012a) and (b) schematic diagram of a physical model considering saturated and unsaturated flows.

is calculated in the solution section), and the flow and water volume should be evaluated based on the second condition. Therefore, the following content will be carried out from the second condition.

Based on the theory presented in Dan et al. (2012a, 2013), the governing equation for transient unsaturated flow in the drainage layer for the second condition can be given by

$$\underbrace{\frac{\partial}{\partial t} \left\{ \underbrace{\phi[H(x, t) - (D - x) \tan \alpha]}_{\text{water content in saturated zone}} + \underbrace{\int_{H(x, t)}^{(D-x)\tan\alpha+T} \theta(\psi) dz}_{\text{water content in unsaturated zone}} \right\}}_{\text{water content change in saturated and unsaturated zone}} = \tag{1}$$

$$\underbrace{\frac{\partial}{\partial x} \left\{ \underbrace{K_S[H(x, t) - (D - x) \tan \alpha] \frac{\partial H(x, t)}{\partial x}}_{\text{flow in saturated zone}} + \underbrace{\int_{H(x, t)}^{(D-x)\tan\alpha+T} K(\psi) dz \cdot \frac{\partial H(x, t)}{\partial x}}_{\text{flow in unsaturated zone}} \right\}}_{\text{flow change in saturated and unsaturated zone}},$$

where K_S is the saturated hydraulic conductivity of the drainage layer [LT^{-1}]; K is the effective hydraulic conductivity [LT^{-1}] (it is defined as the volume of water released from an unconfined aquifer per unit surface area and per unit decline of the water table.); ψ is the capillary pressure head [L]; $H(x, t)$ is the height of the water table above the impermeable base [L]; ϕ is the specific yield of drainage [-] (it is replaced by the effective porosity of drainage layer in this paper); D is the width of the drainage layer [L]; α is the slope of the drainage layer [rad]; T is the thickness of the drainage layer [L]. The second term on the left side in Equation (1) is different from that in Dan’s research (2013) which neglects the nonlinear relationship between hydraulic conductivity and saturation. Based on the Dupuit-Forchheimer assumption that flow is horizontal (Bear & Verruijt, 1987; Dan et al., 2013; Kong, Shen, Luo, Hua, & Zhao, 2016; Youngs & Rushton, 2009), the unsaturated flow can be added into the saturated flow directly and the total hydraulic head can be given by the sum of the suction (negative) head and the elevation head. In this paper, Gardner-type functions (Gardner, 1958; Mualem, 1978) were used, which are in a relatively simple form, in order to derive analytical solutions for the modified model,

$$\begin{cases} \theta = \phi \exp(\alpha_G \psi), \\ K = K_S \exp(\beta_G \psi), \end{cases} \tag{2}$$

where α_G is a constant parameter in Gardner’s model, and the inverse of the mean capillary rise [L^{-1}]; β_G is a parameter accounting for the nonlinear relationship between the saturation and unsaturated hydraulic conductivity. If $\alpha_G = \beta_G$, it means the relationship is linear.

Thus, we have

$$\underbrace{\phi \{1 - \exp[\alpha_G(H(x, t) - (D - x) \tan \alpha - T)]\} \frac{\partial H(x, t)}{\partial t}}_{\text{water content change in saturated and unsaturated zone}} = \tag{3}$$

$$\underbrace{\frac{\partial}{\partial x} \left\{ \underbrace{K_S[H(x, t) - (D - x) \tan \alpha] \frac{\partial H(x, t)}{\partial x}}_{\text{flow in saturated zone}} + \underbrace{K_S \frac{1 - \exp[\beta_G(H(x, t) - (D - x) \tan \alpha - T)]}{\beta_G} \frac{\partial H(x, t)}{\partial x}}_{\text{flow in unsaturated zone}} \right\}}_{\text{flow change in saturated and unsaturated zone}}.$$

2.2. Analytical solution

Here, in order to simplify the expression of the governing equation, $\eta(x, t)$ is defined as

$$\eta(x, t) = H(x, t) - (D - x) \tan \alpha. \tag{4}$$

Accordingly, the following equations hold,

$$\begin{cases} \frac{\partial \eta(x, t)}{\partial x} = \frac{\partial H(x, t)}{\partial x} + \tan \alpha \\ \frac{\partial \eta(x, t)}{\partial t} = \frac{\partial H(x, t)}{\partial t} \\ \frac{\partial^2 \eta(x, t)}{\partial x^2} = \frac{\partial^2 H(x, t)}{\partial x^2}. \end{cases} \tag{5}$$

It is reasonable to linearise Equation (3) in terms of the variable x so that the average thickness of saturated flow is defined as

$$\bar{\eta}(t) = \frac{\int_0^D \eta(x, t) dx}{D}. \tag{6}$$

Substitutions of Equations (4)–(6) into Equation (1) and combination of Equation (5) give

$$\{1 - \exp[\alpha_G(\bar{\eta}(t) - T)]\} \frac{\partial H(x, t)}{\partial t} = \frac{K_S}{\phi} \left\{ \bar{\eta}(t) + \frac{1 - \exp[\beta_G(\bar{\eta}(t) - T)]}{\beta_G} \right\} \frac{\partial^2 H(x, t)}{\partial x^2}, \tag{7}$$

$$\frac{\partial H(x, t)}{\partial t} = \frac{K_S}{\phi} \left\{ \frac{\bar{\eta}(t)}{1 - \exp[\alpha_G(\bar{\eta}(t) - T)]} + \frac{1 - \exp[\beta_G(\bar{\eta}(t) - T)]}{1 - \exp[\alpha_G(\bar{\eta}(t) - T)]\beta_G} \right\} \frac{\partial^2 H(x, t)}{\partial x^2}, \tag{8}$$

where

$$\bar{\eta}(t) = \frac{\int_0^D [H(x, t) - (D - x) \tan \alpha] dx}{D} = \frac{\int_0^D H(x, t) dx}{D} - \frac{1}{2} D \tan \alpha. \tag{9}$$

Due to the difficulty of solving the governing equation of transient unsaturated flow, boundary assumptions are made to simplify the governing equation. It is assumed that the water table at the outlet suddenly drops down to zero and is sustained when the drainage process begins after a rainfall event (Bakker, 2004; Verhoest & Troch, 2000). It avoids the difficulty of moving the boundary due to the changeable height of the seepage face. Therefore, the following conditions can be given:

$$\begin{aligned} \left. \frac{\partial H(x, t)}{\partial x} \right|_{x=0} &= 0 \quad t > 0 \\ H(x, t)|_{x=D} &= 0 \quad t > 0. \end{aligned} \tag{10}$$

The water table varies from the initial water table under the steady state condition when the following drainage process begins, and the height of the initial water table can be expressed as

$$H(x, t)|_{t=0} = H(x), \tag{11}$$

while the height of the initial water table of “time-to-drain” (drainage layer was initially water-saturated) can be expressed as

$$H(x, t)|_{t=0} = (D - x) \tan \alpha + T. \tag{12}$$

2.2.1. Water table distribution

Based on the methods presented (method of separation variables) in Gardner (1962), Gureghian (1978), Srivastava and Yeh (1991), Serrano and Workman (1998), Hogarth, Parlange, Parlange, and Lockington (1999), Smith (2002), Li et al. (2005) and Dan et al. (2013), the product of two functions is assumed to express the solution of the water table as follows:

$$H(x, t) = F(x) \cdot \bar{H}(t), \tag{13}$$

where $F(x)$ is a function of x only and $\bar{H}(t)$ is the average water table and it is a function of t only, and can be denoted by

$$\bar{H}(t) = \frac{\int_0^D H(x, t) dx}{D}. \tag{14}$$

Define that

$$\frac{\bar{\eta}(t)}{1 - \exp[\alpha_G(\bar{\eta}(t) - T)]} + \frac{1 - \exp[\beta_G(\bar{\eta}(t) - T)]}{1 - \exp[\alpha_G(\bar{\eta}(t) - T)]\beta_G} = R(t) + E, \tag{15}$$

where

$$R(t) = \frac{\bar{\eta}(t)}{\alpha_G[T - \bar{\eta}(t)]} \tag{16}$$

and

$$E = \frac{1 - \exp[\beta_G(\bar{\eta}(t) - T)]}{1 - \exp[\alpha_G(\bar{\eta}(t) - T)]\beta_G}. \tag{17}$$

It can be seen that $R(t)$ can be regarded as the flow term dominated by the saturated zone and is affected slightly by the unsaturated zone, while E is treated as the flow term and it is mainly controlled by unsaturated parameters of the drainage material. In order to make derivation simpler, the average water table is neglected simultaneously in the numerator and denominator of Equation (17); thus, we have

$$\frac{1 - \exp[\beta_G(\bar{\eta}(t) - T)]}{1 - \exp[\alpha_G(\bar{\eta}(t) - T)]\beta_G} \approx \frac{1 - \exp(-T\beta_G)}{[1 - \exp(-T\alpha_G)]\beta_G}. \tag{18}$$

It can be seen that if $\alpha_G = \beta_G$, $E = (1/\alpha_G) = (1/\beta_G)$ which can be regarded as the mean thickness of capillary raise [L]; when $\alpha_G \neq \beta_G$, E depends not only on α_G and β_G , but also on the thickness of the drainage layer (T), namely, the area of the vadose zone.

Substituting Equations (16) and (17) into Equation (8) gives

$$\frac{K_s}{\phi} \frac{d^2F(x)/dx^2}{F(x)} = \frac{d[\bar{\eta}(t)]/dt}{\left[\frac{\bar{\eta}(t)}{\alpha_G[T - \bar{\eta}(t)]} + E \right] \cdot \bar{\eta}(t)} = -\omega^2. \tag{19}$$

According to Equation (9), Equation (19) can be rewritten as

$$\frac{K_s}{\phi} \frac{d^2F(x)/dx^2}{F(x)} = \frac{d[\bar{H}(t)]/dt}{\left\{ \frac{\bar{H}(t) - \frac{1}{2}D \tan \alpha}{\alpha_G \left[T + \frac{1}{2}D \tan \alpha - \bar{H}(t) \right]} + E \right\} \cdot \bar{H}(t)} = -\omega^2. \tag{20}$$

It is noted that the introduced parameter (eigenvalue) ω (ω is a positive real number) must be independent of the position from the first ratio and independent of the time from the second ratio.

Then, the expression of $F(x)$ can be given by

$$F(x) = C_1 \sin(\beta x) + C_2 \cos(\beta x), \tag{21}$$

in which $\beta = \omega\sqrt{\phi/K_S}$.

From the boundary conditions that $F'(0) = 0$ and $F(D) = 0$, we have $C_1 = 0$ and $\beta_k = ((2k - 1)\pi)/2D$; thus, $\omega_k = ((2k - 1)\pi)/2D\sqrt{K_S/\phi}$. Accordingly, the following equations can be obtained

$$F_k(x) = C_{2k} \cos \left[\frac{(2k - 1)\pi x}{2D} \right]. \tag{22}$$

According to Equation (13), the following equation holds:

$$\int_0^D H dx = \int_0^D F(X) dx \cdot \bar{H} = \bar{H}. \tag{23}$$

Thus,

$$\int_0^D F(x) dx = 1. \tag{24}$$

On the basis of Equation (22), the following equation holds:

$$\int_0^D F_k(x) dx = C_{2k} \int_0^D \cos \left[\frac{(2k - 1)\pi x}{2D} \right] dx = 1. \tag{25}$$

Thus, we have

$$C_{2k} = (-1)^{k-1} \cdot \frac{(2k - 1)\pi}{2} \tag{26}$$

and

$$F_k(x) = \frac{(2k - 1)\pi}{2(-1)^{k-1}} \cos \left[\frac{(2k - 1)\pi x}{2D} \right]. \tag{27}$$

Furthermore, the following equation can be obtained according to Equation (20),

$$A \ln(\bar{H}_k) - B\bar{H}_k = -\omega_k^2 t + C_{3k}, \tag{28}$$

where

$$A = \frac{1}{E} + \frac{D \tan \alpha}{2TE} \quad \text{and} \quad B = \frac{1}{TE}. \tag{29}$$

By solving Equation (28), it gives

$$\bar{H}_k = -\frac{A}{B} \text{LambertW} \left[-\frac{B}{A} \exp \left(\frac{-\omega_k^2 t + C_{3k}}{A} \right) \right], \tag{30}$$

in which Lambert W is the so-called Lambert W function, and the W_0 branch is used for calculation in this paper.

Therefore,

$$H_k(x, t) = \frac{A}{B} \sum_{k=1}^{\infty} \frac{(2k-1)\pi}{2(-1)^k} \cos \left[\frac{(2k-1)\pi}{2} \frac{x}{D} \right] \cdot \text{LambertW} \left[-\frac{B}{A} \exp \left(\frac{-\omega_k^2 t + C_{3k}}{A} \right) \right] \quad (31)$$

and

$$H(x, t) = \sum_{k=1}^{\infty} H_k(x, t). \quad (32)$$

From the initial condition, we have

$$H(x, 0) = \frac{A}{B} \sum_{k=1}^{\infty} \frac{(2k-1)\pi}{2(-1)^k} \cos \left[\frac{(2k-1)\pi}{2} \frac{x}{D} \right] \cdot \text{LambertW} \left[-\frac{B}{A} \exp \left(\frac{C_{3k}}{A} \right) \right] = H(x). \quad (33)$$

In view of the orthogonality of trigonometric functions, we have

$$\begin{aligned} & \frac{A}{B} \sum_{k=1}^{\infty} \left\{ \frac{(2k-1)\pi}{2(-1)^k} \cdot \text{LambertW} \left[-\frac{B}{A} \exp \left(\frac{C_{3k}}{A} \right) \right] \right\} \int_0^D \cos \left[\frac{(2k-1)\pi}{2} \frac{x}{D} \right] \cos \left[\frac{(2j-1)\pi}{2} \frac{x}{D} \right] dx \\ &= \int_0^D H(x) \cos \left[\frac{(2j-1)\pi}{2} \frac{x}{D} \right] dx \\ &= \frac{A}{B} \sum_{k=1}^{\infty} \left\{ \frac{(2k-1)\pi}{2(-1)^k} \cdot \text{LambertW} \left[-\frac{B}{A} \exp \left(\frac{C_{3k}}{A} \right) \right] \right\} \frac{D}{2} \delta_{k,j} \\ &= \frac{DA}{2B} \left\{ \frac{(2k-1)\pi}{2(-1)^k} \cdot \text{LambertW} \left[-\frac{B}{A} \exp \left(\frac{C_{3k}}{A} \right) \right] \right\} \end{aligned} \quad (34)$$

where $\delta_{k,j}$ is a function and given by

$$\delta_{k,j} = \begin{cases} 0 & k \neq j, \\ 1 & k = j. \end{cases} \quad (35)$$

Thus,

$$\begin{aligned} & \frac{A}{B} \sum_{k=1}^{\infty} \left\{ \frac{(2k-1)\pi}{2(-1)^k} \cdot \text{LambertW} \left[-\frac{B}{A} \exp \left(\frac{C_{3k}}{A} \right) \right] \right\} \frac{D}{2} \delta_{k,j} \\ &= \frac{DA}{2B} \left\{ \frac{(2k-1)\pi}{2(-1)^k} \cdot \text{LambertW} \left[-\frac{B}{A} \exp \left(\frac{C_{3k}}{A} \right) \right] \right\} = \int_0^D H(x) \cos \left[\frac{(2k-1)\pi}{2} \frac{x}{D} \right] dx. \end{aligned} \quad (36)$$

If the initial condition is that the drainage layer is fully saturated in a certain case (the assumption of the time-to-drain method), the initial condition for these types of cases is given in Equation (12), and accordingly we have

$$\int_0^D H(x) \cos \left[\frac{(2k-1)\pi}{2} \frac{x}{D} \right] dx = \frac{D}{\left[\frac{(2k-1)\pi}{2} \right]^2} \left[D \tan \alpha + \frac{(2k-1)\pi}{2} T(-1)^{k-1} \right]. \quad (37)$$

Combining Equations (36) and (37), the following equation holds:

$$-\text{LambertW} \left[-\frac{B}{A} \exp \left(\frac{C_{3k}}{A} \right) \right] = \frac{B}{A} \frac{8\sigma(k)}{[(2k-1)\pi]^2} \quad (38)$$

where

$$\sigma(k) = T + \frac{D \tan \alpha}{(2k-1)\pi} (-1)^{k-1}. \tag{39}$$

Accordingly, Equation (38) can be solved and

$$C_{3k} = A \ln \left\{ \frac{8\sigma(k)}{[(2k-1)\pi]^2} \right\} - B \frac{8\sigma(k)}{[(2k-1)\pi]^2}. \tag{40}$$

Combining Equations (26), (29), (32), (39) and (40), the solution of the water table in terms of time can be expressed by

$$H(x, t) = - \left(T + \frac{1}{2} D \tan \alpha \right) \sum_{k=1}^{\infty} \frac{(2k-1)\pi}{2} (-1)^{k-1} \cos \left[\frac{(2k-1)\pi}{2} \frac{x}{D} \right] \cdot \text{LambertW}(\xi_k) \tag{41}$$

with

$$\xi_k = - \frac{1}{T + \frac{1}{2} D \tan \alpha} \exp \left(- \frac{\omega_k^2 E t}{1 + \frac{D \tan \alpha}{2T}} + \ln \left\{ \frac{8\sigma(k)}{[(2k-1)\pi]^2} \right\} - \frac{1}{T + \frac{1}{2} D \tan \alpha} \frac{8\sigma(k)}{[(2k-1)\pi]^2} \right). \tag{42}$$

When $\tan \alpha = 0$, a special case is obtained for the water table (H), i.e.

$$H(x, t) = - \left(T + \frac{1}{2} D \tan \alpha \right) \sum_{k=1}^{\infty} \frac{(2k-1)\pi}{2} (-1)^{k-1} \cos \left[\frac{(2k-1)\pi}{2} \frac{x}{D} \right] \cdot \text{LambertW}(\xi_k) \tag{43}$$

with

$$\xi_k = - \frac{1}{T} \exp \left(- \omega_k^2 E t + \ln \left\{ \frac{8T}{[(2k-1)\pi]^2} \right\} - \frac{8}{[(2k-1)\pi]^2} \right). \tag{44}$$

Furthermore, when the parameter E is very small (it means the values of α_G and β_G in Equation (17) are very large), the drainage process can be degenerated to a saturated case, and the solution is still valid.

2.2.2. Water storage

Generally, because it is assumed that the drainage layer is fully saturated in the initial state, the water volume can be easily obtained. During the drainage process, the calculation of water storage in a sloping drainage layer can be divided into two scenarios, which depends on the water table distribution.

The first scenario is that the water table is below the top of the drainage layer. The water volume in the drainage layer including the unsaturated zone and the saturated zone can be evaluated as follows according to the general solution:

$$V(t) = \phi \int_0^D \left\{ H(x, t) - (D - x) \tan \alpha + \frac{1 - \exp[\alpha_G(H(x, t) - (D - X) \tan \alpha - T)]}{\alpha_G} \right\} dx. \tag{45}$$

The second scenario is that the water table is partially below the bottom of the drainage layer. The water storage can be evaluated by

$$\begin{cases} V(t) = \phi \int_0^{x_1} \left\{ \frac{\exp\{\alpha_G[H(x, t) - (D - x) \tan \alpha]\} - \exp\{\alpha_G[H(x, t) - (D - x) \tan \alpha - T]\}}{\alpha_G} \right\} dx \\ \quad \text{if } H(x, t) < (D - x) \tan \alpha, \\ V(t) = \phi \int_{x_1}^D \left\{ H(x, t) - (D - x) \tan \alpha + \frac{1 - \exp[\alpha_G(H(x, t) - (D - x) \tan \alpha - T)]}{\alpha_G} \right\} dx \\ \quad \text{if } H(x, t) > (D - x) \tan \alpha, \end{cases} \tag{46}$$

in which x_1 is the intersection point of the drainage layer bottom and the calculated water table height. x_1 can be calculated numerically according to the water table distribution by

$$H(x, t) = (D - x) \tan \alpha. \tag{47}$$

For Equation (45),

$$V(t) = \phi \int_0^D \left\{ H(x, t) - (D - x) \tan \alpha + \frac{1 - \exp[\alpha_G(H(x, t) - (D - x) \tan \alpha - T)]}{\alpha_G} \right\} dx, \tag{48}$$

$$\begin{aligned} V(t) &= \phi \int_0^D H(x, t) dx - \phi \int_0^D [(D - x) \tan \alpha] dx \\ &\quad + \phi \int_0^D \left\{ \frac{1 - \exp[\alpha_G(H(x, t) - (D - x) \tan \alpha - T)]}{\alpha_G} \right\} dx, \end{aligned} \tag{49}$$

$$V(t) = \phi \left(D\bar{H} - \frac{1}{2}D^2 \tan \alpha + \frac{D}{\alpha_G} - \frac{\exp[\alpha_G(\bar{H} - T)] - \exp[\alpha_G(\bar{H} - D \tan \alpha - T)]}{\alpha_G^2 \tan \alpha} \right), \tag{50}$$

$$\bar{H}(t) = \frac{\int_0^D H(x, t) dx}{D} = -2 \left(T + \frac{1}{2}D \tan \alpha \right) \sum_{k=1}^{\infty} \frac{(-1)^{k-1} C_{2k} \cdot \text{LambertW}(\xi_k)}{(2k - 1)\pi}. \tag{51}$$

For Equation (46) and the case $H(x, t) > (D - x) \tan \alpha$, the water volume can be calculated by

$$\begin{aligned} V(t) &= \phi \int_{x_1}^D H(x, t) dx - \phi \int_{x_1}^D [(D - x) \tan \alpha] dx \\ &\quad + \phi \int_{x_1}^D \left\{ \frac{1 - \exp[\alpha_G(H(x, t) - (D - x) \tan \alpha - T)]}{\alpha_G} \right\} dx. \end{aligned} \tag{52}$$

Thus,

$$\begin{aligned} V(t) &= \phi \left((D - x_1)\bar{H}^* - \frac{1}{2}(D - x_1)^2 \tan \alpha \right. \\ &\quad \left. + \frac{D - x_1}{\alpha_G} - \frac{\exp[\alpha_G(\bar{H} - T)] - \exp[\alpha_G(\bar{H} - (D - x_1) \tan \alpha - T)]}{\alpha_G^2 \tan \alpha} \right) \end{aligned} \tag{53}$$

Table 1. Calculation parameters.

T (m)	D (m)	$\alpha_G = \beta_G$ (m ⁻¹)	$\tan \alpha$	K_S (m/s)	ϕ
0.1	10	7.05	0.02	0.00463	0.2

in which

$$\begin{aligned} \overline{H^*}(t) &= \frac{\int_{x_1}^D H(x, t) dx}{D - x_1} \\ &= -\frac{2D(T + \frac{1}{2}D \tan \alpha)}{D - x_1} \sum_{k=1}^{\infty} \frac{\left\{ (-1)^{k-1} - \sin \left[\frac{(2k-1)\pi}{2} \frac{x_1}{D} \right] \right\} C_{2k} \cdot \text{LambertW}(\xi_k)}{(2k - 1)\pi}. \end{aligned} \tag{54}$$

For Equation (46) and the case $H(x, t) < (D - x) \tan \alpha$, the water volume can be expressed by

$$V(t) = \phi \left\{ \frac{\exp\{\alpha_G[\overline{H^{**}}(t) - (D - x) \tan \alpha]\}_{x_1}^{x_1} - \exp\{\alpha_G[\overline{H^{**}}(t) - (D - x) \tan \alpha - T]\}_{0}^{x_1}}{\alpha_G^2 \tan \alpha} \right\}, \tag{55}$$

$$\overline{H^{**}}(t) = \frac{\int_0^{x_1} H(x, t) dx}{x_1} = -\frac{2D(T + \frac{1}{2}D \tan \alpha)}{x_1} \sum_{k=1}^{\infty} \frac{\sin \left[\frac{(2k-1)\pi}{2} \frac{x_1}{D} \right] C_{2k} \cdot \text{LambertW}(\xi_k)}{(2k - 1)\pi}. \tag{56}$$

3. Model validation

In this section, the accuracy of the analytical solution is validated against the finite-element solutions. We compare the present analytical solution with a 2-D Richards equation-based model (Richards, 1931) (the Richards equation which represents the movement of water in unsaturated soils was formulated by Richards in 1931), SUTRA (a finite element computer program that simulates partially saturated pore-water flow (Voss & Provost, 2008)). Based on the SUTRA, we solved Equation (1) using the same boundary conditions and the same water retention curve as used in the analytical solution. Therefore, the key difference between the analytical solution and the SUTRA was that the former considered the linear approximation to the 2-D Richards equation. The parameters used in the calculations are listed in Table 1. Five conditions were considered that $t = 0, 30, 60, 90$ and 120 min. It can be seen from Figure 2 that the present analytical solution and the SUTRA predict similar results in terms of the water table. In addition, when $\alpha = 0$, the solution will degenerate to a similar condition as in Xin’s research (2016) which was validated by the experiment.

This demonstrated that the linear approximation to the 2-D Richards equation is reasonable for the drainage system with shallow water tables. In comparison with the Richards equation-based model, the present analytical solution is relatively simple and straightforward, and would favour process understanding and practical applications.

4. Effect analysis and discussion

A sensitivity analysis was conducted to quantify the importance of the effects of material properties and geometric dimension of the drainage layer for guiding design of the drainage layer.

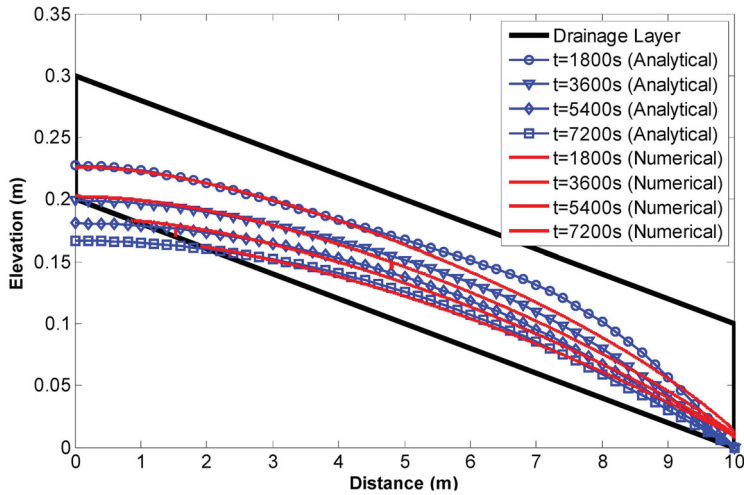


Figure 2. Prediction of water table distribution for various drainage times by using both analytical and numerical methods.

4.1. Time to drain water volume

In order to quantify the drainage capacity of the drainage layer, the ratio of drained water volume to the initial water volume (the initial water content V_i is saturated throughout the drainage layer) was defined by W_D (drainage ratio) in Equation (56), in which V_{t_D} is the water volume at time t_D ,

$$\frac{V_i - V_{t_D}}{V_i} \times 100\% = W_D. \tag{57}$$

Casagrande and Shannon, and USACE (The United States Army Corps of Engineers) suggested that the time to drain 50% water volume should not be longer than 10 days (Casagrande & Shannon, 1952). This kind of criterion is not suitable for the current heavy traffic. Barksdale and Hicks recommended that it should take 2 to 6 hours to drain 50% water (AASHTO, 1993). AASHTO (1993) also ranked four classifications of drainage performance as excellent, good, fair, poor and very poor according to the drainage time which is shown in Table 2. In order to show the drainage process, based on Equations (46)–(56), the ratio (W_D) of the drained water volume to the initial water volume (the total volume of the initial water content in the saturated per unit width according to the assumption of the time-to-drain method) in the drainage layer was calculated and is illustrated in Figure 3 and the parameters are listed in Table 1. It can be seen that the relationship between the ratio (W_D) and elapsed drainage time is obviously nonlinear. Further, the drainage process lasts much too long as a whole; however, only about 62% water can be drained by the drainage layer up to 80 hours (about 3.4 days), and the drainage is not obvious after 30 hours in Figure 3. The time to drain 50% water volume is about 11.68, and the classification of drainage performance can be ranked as good according to Table 2.

According to the solutions, the geometric dimension of the drainage layer (slope, thickness and width), the hydraulic conductivity and the water retention curve-related parameters such as α_G and β_G are the factors affecting the drainage process. Therefore, the detailed analysis will be conducted as follows.

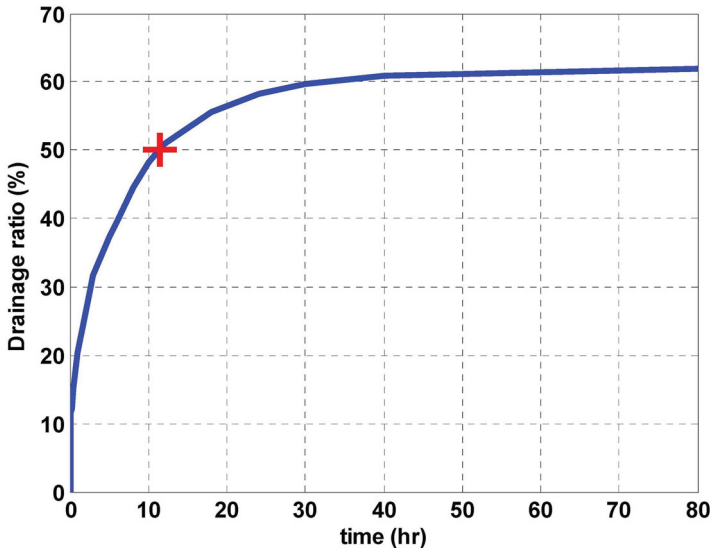


Figure 3. Drainage ratio vs. time.

Table 2. Classification of drainage performance (AASHTO, 1993).

Drainage rank	Time to drain 50% water
Excellent	2 hours
Good	2 days
Fair	1 week
Poor	1 month
Very poor	> 1 month

Table 3. Calculation scenarios.

$\phi = 0.2, \tan \alpha = 0.02T = 0.1 \text{ m}, D = 10 \text{ m}, K_S = \frac{\lambda\phi}{E} [\text{cm/s}]$		$\alpha_G = \beta_G = \frac{1}{E} (\text{m}^{-1})$			
		10	20	40	80
$\lambda = \frac{K_S E}{\phi} (\text{m}^2/\text{s})$	2.5×10^{-4}	0.05	0.1	0.2	0.4
	5.0×10^{-4}	0.1	0.2	0.4	0.8
	1.0×10^{-3}	0.2	0.4	0.8	1.6
	2.0×10^{-3}	0.4	0.8	1.6	3.2
	3.0×10^{-3}	0.6	1.2	2.4	4.8
	4.0×10^{-3}	0.8	1.6	3.2	6.4

4.2. Effect of drainage material

It can be seen from the calculation expressions (e.g. Equations (41) and (45)) that the water table and water storage (changing with time) depend on the geometric parameters and drainage material. It means that when the slope, thickness and wideness of the drainage layer are determined, the time-dependent drainage ratio is dependent on hydraulic conductivity, porosity and the unsaturated properties of the material. Here, we defined a comprehensive parameter for representing

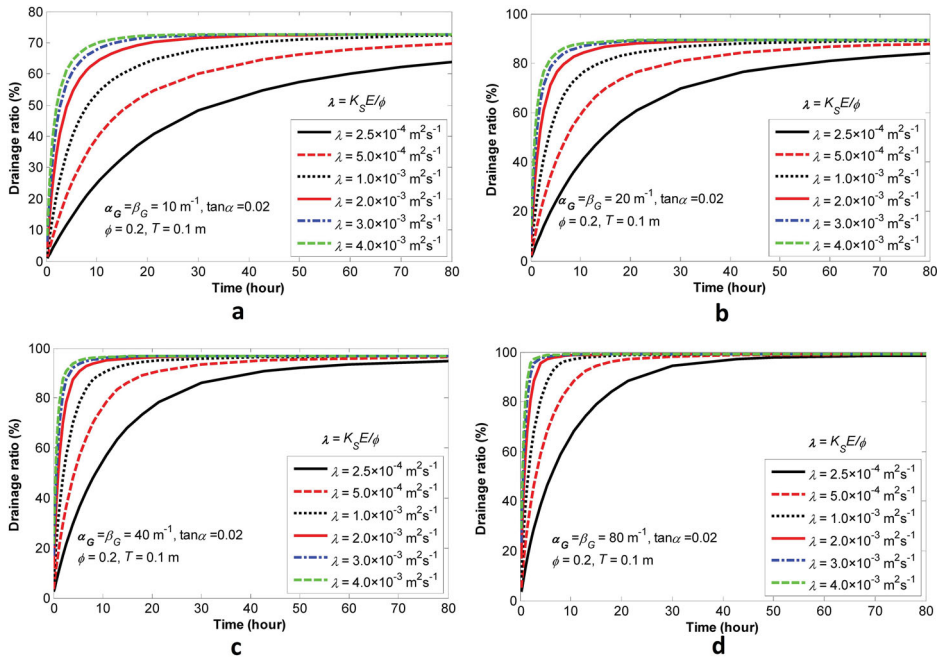


Figure 4. Drainage ratio vs. time for various calculation conditions.

the hydraulically related property of the drainage layer,

$$\lambda = \frac{K_S E}{\phi} \tag{58}$$

According to Equation (58), it can be inferred that λ depends on the saturated hydraulic conductivity, porosity and E (if $\alpha_G = \beta_G$, E is the inverse of α_G). In practical engineering, the value of λ does not change obviously to some extent. Commonly, the porosity of the drainage layer does not change obviously in pavement engineering; thus the porosity is not taken into account in this paper. Therefore, in order to test the effect of the drainage material, the following scenarios are taken into account, shown in Table 3 (large value of α_G represents coarser drainage material). The effect of hydraulic conductivity is incorporated based on Equation (58). The calculation results are shown in Figure 4 and Figure 5.

Figure 4 shows the drainage process of the drainage layer, and it can be seen that the drainage ratio increases with time nonlinearly in the same manner for different scenarios. When α_G remains constant, the drainage speed accelerates with increase in λ . Quantitatively, when $\alpha_G = 10\text{m}^{-1}$, and λ varies from $1.0 \times 10^{-3} \text{m}^2/\text{s}$ to $4.0 \times 10^{-3} \text{m}^2/\text{s}$, the time to drain 50% water is 8.16, 4.09, 2.74 and 2.04 hours. Moreover, for larger α_G (smaller value of E), the final drainage ratio is higher. That is to say, more residual water cannot drain out during the calculation time. For the same α_G and different λ , which means different saturated hydraulic conductivity, however, the final drainage ratio can reach the same value. For instance, when λ varies from $1.0 \times 10^{-3} \text{m}^2/\text{s}$ to $4.0 \times 10^{-3} \text{m}^2/\text{s}$ (saturated hydraulic conductivity changes from 0.4 cm/s to 1.6 cm/s) and $\alpha_G = 20\text{m}^{-1}$, all of the final ratios are about 89%; while $\alpha_G = 80\text{m}^{-1}$, the final ratio approximates to be 100%.

Based on the above-mentioned results, it can be inferred that the final drainage ratio depends on α_G rather than λ or saturated hydraulic conductivity (K_S). Nevertheless, the drainage speed is

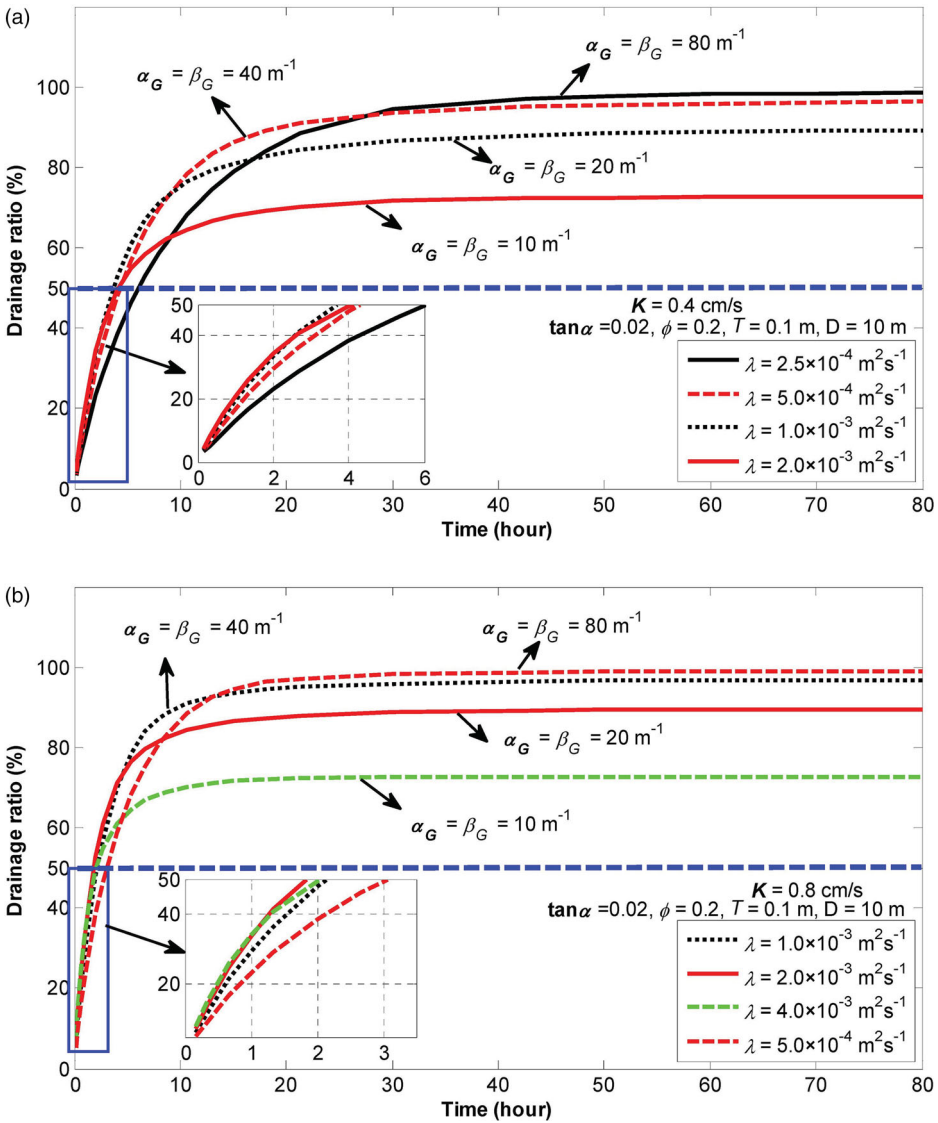


Figure 5. (a) Drainage ratio vs. time for $K_S = 0.4$ cm/s under condition of various α_G and β_G and (b) drainage ratio vs. time for $K_S = 0.8$ cm/s under condition of various α_G and β_G .

affected by hydraulic conductivity obviously. For example, when $\alpha_G = \beta_G = 20\text{m}^{-1}$ and varies from $1.0 \times 10^{-3} \text{ m}^2/\text{s}$ to $4.0 \times 10^{-3} \text{ m}^2/\text{s}$ (saturated hydraulic conductivity changes from 0.4 to 1.6 cm/s), the time to drain 50% water volume is 3.67, 1.83, 1.22 and 0.92 hours, respectively.

For the same hydraulic conductivity case which is shown in Figure 5(a) and (5b), the early drainage speed is higher for a case of lower value of α_G , and the final drainage ratio is larger for a case of higher value of α_G . Overall, the drainage times of 50% water are almost approximated for α_G and are 10m^{-1} , 20m^{-1} and 40m^{-1} (drainage time is about 2 hours for the case of $K_S = 0.8$ cm/s and 4 hours for the case of $K_S = 0.4$ cm/s) except for that of 80m^{-1} (drainage time is about 3.2 hours for the case of $K_S = 0.8$ cm/s and 6 hours for the case of $K_S = 0.4$ cm/s). According to the classification of drainage performance, the former scenario when α_G are 10m^{-1} ,

20m⁻¹ and 40m⁻¹ can be ranked as excellent, while it is ranked as good when α_G is 80m⁻¹ even though it can drain larger water volume finally. It is known that when α_G is large, the capillary effect is low; however, from the view of material selection, the α_G is better to reach a relative low value, because the low value of α_G is benefit to improve the strength of the drainage layer (Dan, He, & Xu, 2016).

According to the analysis above, the drainage ratio mainly depends on the value of λ . In order to reach a faster drainage speed, a relatively larger value of λ should be maintained. Firstly, higher K_S and lower α_G and porosity (ϕ) are feasible according to Equation (58); however, the hydraulic conductivity is directly proportional and sensitive to the gradation in practice (Dan et al., 2016). In addition, the proportional relationship is basically actual between K_S and α_G . Therefore, how to control these parameters is crucial to design a better drainage layer in terms of drainage properties without considering the mechanical properties of drainage materials (because the higher hydraulic conductivity will lead to reduction of the strength of the drainage layer; on the contrary, the strength of the drainage layer can be improved by reducing the hydraulic conductivity). Based on the above analysis, it is possible to find a reasonable way to improve the drainage efficiency and strength of the drainage layer simultaneously. In other words, we can use lower K_S , ϕ and α_G to reach a higher λ and higher modulus of the drainage layer.

Furthermore, according to Equation (18), we have

$$E \approx \frac{1 - \exp(-T\beta_G)}{[1 - \exp(-T\beta_G)]\beta_G}. \quad (59)$$

According Equation (2), the following equation holds:

$$\begin{cases} K_R = S_e^N, \\ N = \beta_G/\alpha_G, \end{cases} \quad (60)$$

where K_R is the relative hydraulic conductivity [-]; S_e is the effective saturation in the drainage layer [-], and N represents the degree of nonlinear relationship between the hydraulic conductivity and saturation [-]. The various values of N results in different E and λ . The drainage time and drainage ratio will be different. Generally, the range of N does not change largely, and is around 1.0 to 3.0 in soils and sands (Averjanov, 1950; Mualem, 1978), which indicates that the value of β_G is generally larger than α_G . Here, N is assumed to change from 1.0 to 6.0; in this paper, the sensitivity analysis is conducted and the result is shown in Figure 6.

It can be seen that when N increase from 1.0 to 4.0, the values of both E and λ decrease, especially for a smaller α_G ; this kind of reduction is obvious. According to the previous analysis, the excessively low value of λ will lead to a slower drainage speed and make the drainage process last for a longer time. In general, coarser granular material has the property of large value of N . Therefore, determining the gradation of the drainage layer should be considered. A high percentage of large-sized particles in the drainage layer may not lead to a good drainage efficiency. A suitable amount of fine particles is also necessary to reach better drainage performance.

4.3. Effect of slope of the drainage layer

The drainage layer should drain into a longitudinal drainage pipe. In order to encourage the lateral flow of water, a minimum cross-fall should be considered, of at least 2% (Dawson, 2008). In general, the transverse slope of the drainage layer is 2% according to the Chinese design criterion (MOTPRC, 2006; MOTPRC, 2012), and the slope does not change obviously. In order to analyse the effect of slope, several conditions are taken into consideration as shown in Figure 7(a). Obviously, a larger slope can accelerate the drainage process. On the one hand, the time to drain

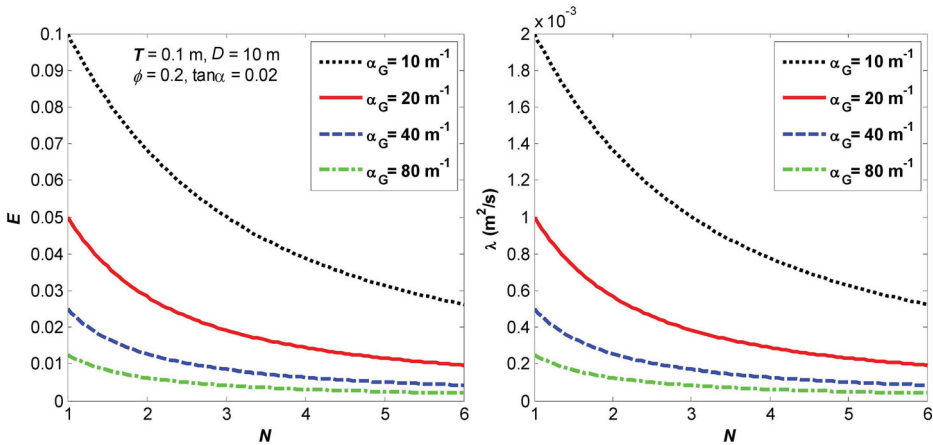


Figure 6. Effect of N (nonlinear degree of hydraulic conductivity with saturation) on E and λ for various α_G .

a specified quantity of water is reduced; on the other hand, the final drainage ratio was raised with increasing slope (Figure 7(b)). For instance, the time to drain 50% water is respectively 5.3, 4.1, 3.4, 2.9, 2.6 and 2.3 hours and the final drainage ratio is respectively 67.3%, 72.7%, 76.8%, 80%, 82.5% and 84.5% when the drainage slopes are 1.5%, 2%, 2.5%, 3%, 3.5% and 4.0%. Therefore, the drainage improvement is distinct when the drainage slope increases. However, the incline degree of the drainage layer is dependent on the transverse slope of the pavement, which is determined according to the design criterion.

4.4. Effect of drainage layer thickness

It is a common practice to provide a drainage layer in subsurface drainage systems in order to remove the infiltrated/seepage water from the pavement structures. Drainage layers should be at least 10–15 cm thick and extend under the full width of the roadway (Dawson, 2008). In this paper, four cases of thickness (T are 0.1 , 0.15 , 0.2 and 0.25 m, the hydraulic conductivity is taken as 0.8 cm/s for calculation) are taken into account in sensitivity analysis, the results of which are shown in Figure 8. It shows that the drainage ratio goes up slightly when the thickness of the drainage layer increases. Alternatively, the effect of drainage layer thickness on the final drainage ratio and time to drain 50% water is not very obvious. For instance, the final drainage ratio is about 89%, 92%, 94% and 95%, and the time to drain 50% water is 1.84, 1.68, 1.59 and 1.51 hours, respectively. That is to say, when the thickness of the drainage layer increases by 2.5 times, the drainage time only reduces about 18%. In addition, for a lower hydraulic conductivity, namely, $K_S = 0.4 \text{ cm/s}$, this kind of effect maintains the same situation. For instance, the time to drain 50% water is 3.67, 3.37, 3.17 and 3.02 hours, respectively, and the drainage time is also reduced by about 18% (Figure 9). In summary, a thicker drainage layer will enhance the drainage process due to the effect of a larger unsaturated zone. Nevertheless, this kind of effect is not distinct. Therefore, it is not practicable to improve the drainage performance by increasing the thickness of a drainage layer because a thicker drainage layer may lead to a much larger deformation of the pavement structure.

4.5. Drainage performance improvement

In order to assist in the design of the drainage layer, the drainage performance is illustrated under different materials' properties. According to Equation (58), three parameters (K_S , E and

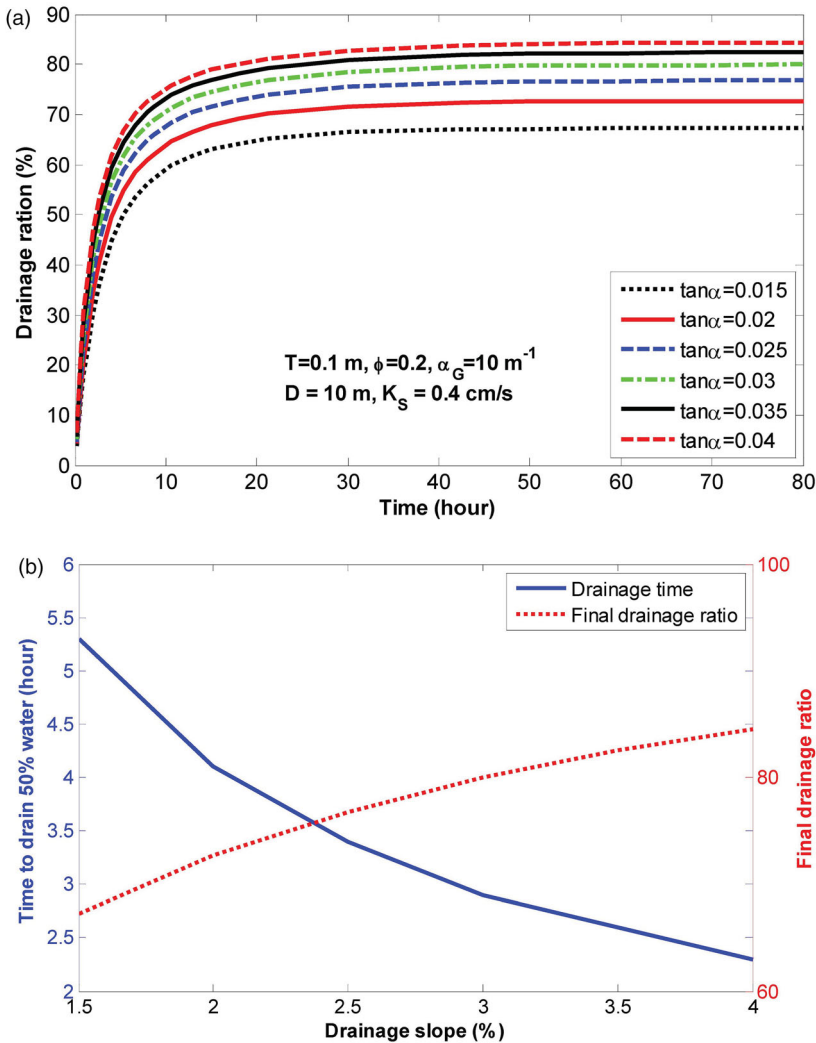


Figure 7. (a) Drainage ratio vs. time for various drainage slopes and (b) effect of drainage slope on time to drain 50% water and final drainage ratio.

ϕ) relate to the drainage performance closely. Based on the above discussions, ϕ does not change obviously; therefore, the analysis herein only focuses on the effects of K_S and E (E is represented by α_G) on the drainage performance. In this paper, the value of K_S varies from 0.1 to 5 cm/s and α_G ranges from 5 to 200 m^{-1} , and $\phi = 0.15$. For other calculation geometrical parameters refer to Table 1. Accordingly, the time to drain 50% water is obtained and ranked based on Table 2 and is shown in Figure 10.

Overall, it can be seen from Figure 10(a) that a majority of combinations of K_S and α_G can reach excellent drainage performance and are distributed on the right-hand side area. On the left side area in Figure 10(a), the drainage performance is lower to good and fair ranks (at the bottom left area). The details are demonstrated in Figure 10(b) and Figure 10(c), respectively.

To better understand the drainage performance, the final drainage ratios for different conditions were calculated and shown in Figure 11. It shows the capacity of the drainage layer to drain

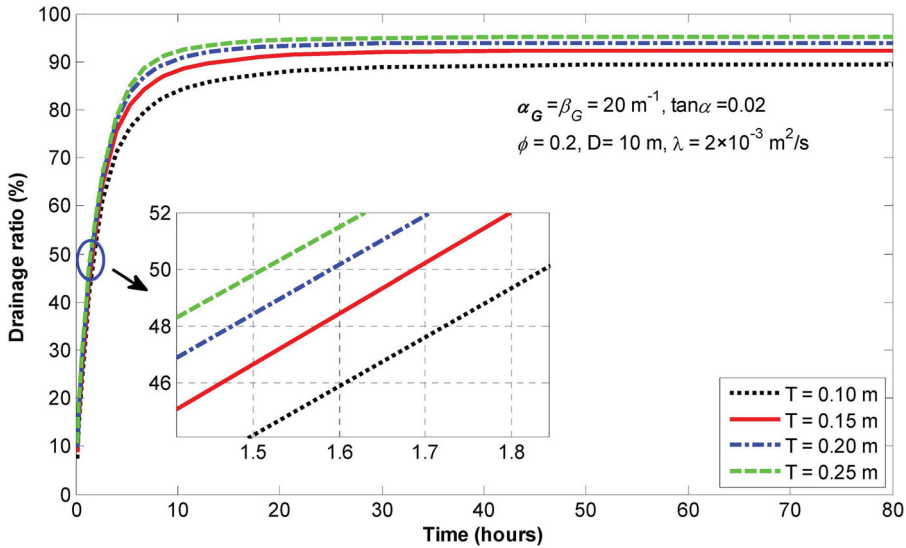


Figure 8. Drainage ratio vs. time for various thicknesses of the drainage layer.

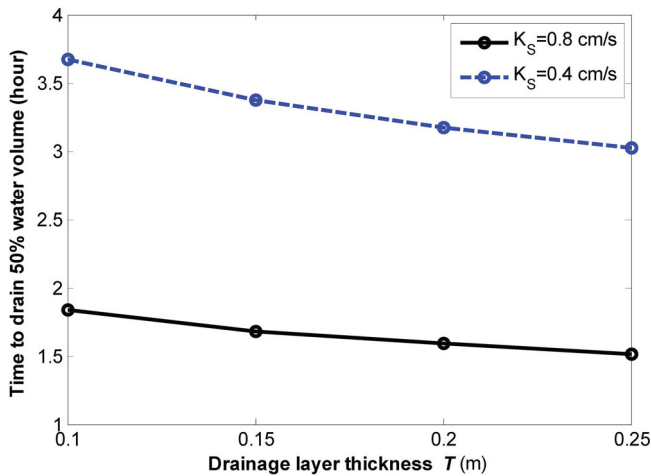


Figure 9. Effect of drainage layer thickness on time to drain 50% water under different permeability conditions.

out the infiltrating water. It also illustrates the residual water left in the drainage layer. In the current drainage design specification, the final drainage ratio is not taken into consideration. For instance, when the value of α_G is very low (e.g. α_G and K_S are 6 m^{-1} and 0.004 m/s respectively), the final drainage ratio cannot reach a higher value (e.g. 52%); it means a large amount of water (48%) is detained in the drainage layer although the drainage performance is ranked as GOOD. It demonstrates the current method is defective to assess the drainage performance. In view of this, the high value of α_G and K_S can be applied to achieve better drainage performance and lower residual water in the drainage layer. By taking into account the strength of the drainage layer, an extremely high value of α_G and K_S may not be the optimum selection for design of the drainage layer due to the reciprocal relationship between drainage performance and strength.

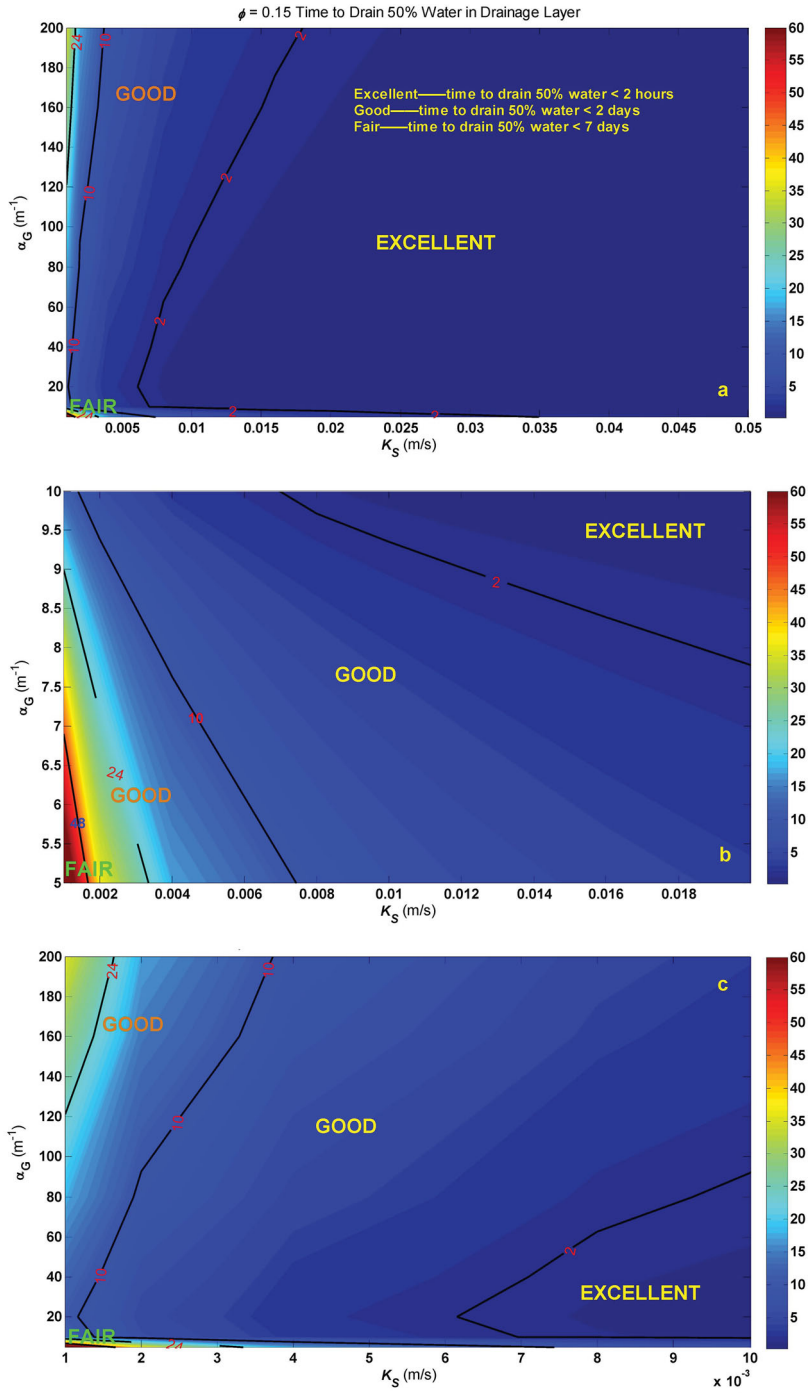


Figure 10. Drainage performance for different drainage materials.

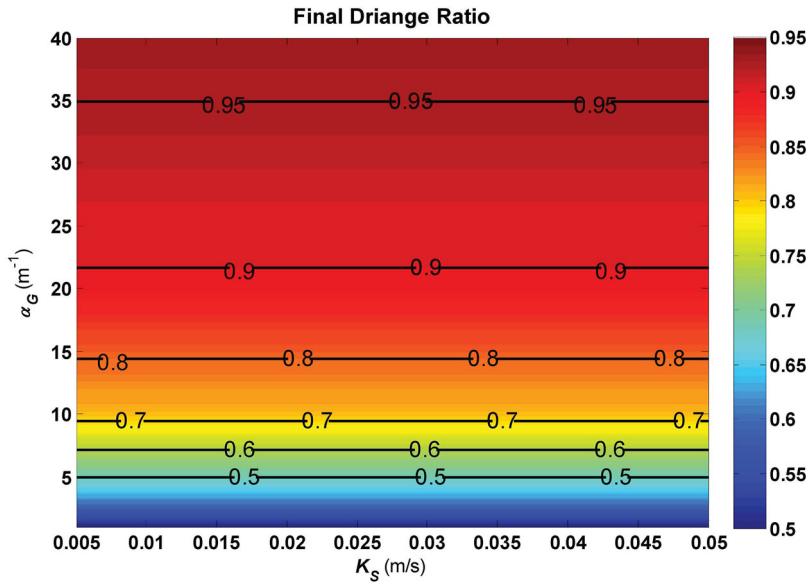


Figure 11. Final drainage ratio for different drainage materials.

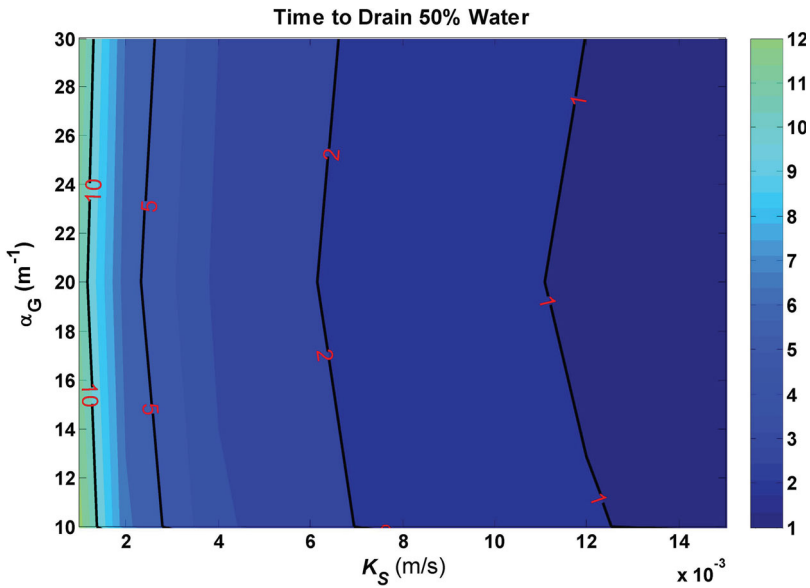


Figure 12. Recommended value of hydraulic parameters for the drainage material.

Therefore, an appropriate value needs to be considered carefully. Herein, according to engineering experience, α_G located in $10 \sim 30 \text{ m}^{-1}$ and K_S change from 0.1 to 1.5 cm/s may be a better selection to guide drainage design (Figure 12). On the one hand, the residual water is low and the drainage performance rank is excellent or close to excellent; on the other hand, the gradation of the drainage layer can accommodate the hydraulic conductivity to satisfy the strength of the drainage layer (Dan et al., 2016).

5. Concluding remarks

This study developed a model to simulate the transient flow in a highway subsurface drainage system based on the concept of “time-to-drain”. The model further incorporated the capillary effect and the nonlinear relationship between hydraulic conductivity and saturation. In this model, both the saturated and the unsaturated dominant terms in the governing equation were presented, and the boundary condition at the flow outlet was simplified with the seepage face neglected to avoid the difficulty of a moving boundary problem. The method of separation variables was then employed to solve the governing equation. To validate the model and the analytical solution, a 2D Richards equation-based model (SUTRA) incorporating the Gardner water retention curve was applied. The comparisons between the analytical and SUTRA results validate the model in predicting the transient height of the water table.

To quantify the drainage performance of the drainage layer, the expression of water volume varying with time during the drainage process was derived, and four classifications were used to rank the drainage performance by incorporating the final drainage ratio. The effect analysis was also carried out to illustrate the effects of the drainage material and geometric parameters on the drainage efficiency. The following conclusions were drawn to facilitate the design of the subsurface drainage system of a highway.

- (1) Drainage time was reduced by capillarity, whereas the drainage efficiency was enhanced by the vadose zone. The final drainage ratio depends on α_G instead of saturated hydraulic conductivity (K_S) or λ . It indicates that the water in the drainage layer can be drained out completely based on the saturated flow-based model (when the value of α_G trends to be infinite) (e.g. Boussinesq equation-based model, Laplace equation-based model) even though the hydraulic conductivity is extremely low. It violates the practical experiment. Therefore, the saturated flow model is not suitable for designing drainage systems of a highway.
- (2) The drainage speed can be improved by rising the hydraulic conductivity of the drainage layer. Nevertheless, for the same hydraulic conductivity case, the early drainage speed is higher for lower α_G , and the final drainage ratio is higher for larger value of α_G . It is known that when α_G is large, the capillary effect is low. Therefore, from the view of material selection, a relatively lower value of α_G helps to improve the strength of the drainage layer. Furthermore, for better drainage, lower values of K_S , ϕ and α_G can be used in order to reach a higher λ and a higher modulus of the drainage layer.
- (3) The nonlinear relationship between hydraulic conductivity and saturation affects the drainage as well. A coarser granular material has the property of larger value of N ; high percentage of large size particle in the drainage layer may not lead to good drainage efficiency. A suitable amount of fine particles is necessary to reach better drainage performance.
- (4) The drainage improvement is significant when the drainage slope increases. However, the incline degree of the drainage layer depends on the transverse slope of the pavement, which is determined according to the design criterion.
- (5) As a whole, larger thickness of drainage layers will enhance the drainage process slightly due to the effect of a larger unsaturated zone. It is impracticable to improve the drainage performance through increasing thickness of the drainage layer due to the reason that a larger drainage layer will generally lead to a larger deformation of the pavement structure.
- (6) According to engineering experience, appropriate values of α_G and K_S were presented for drainage material selection to guide the drainage design. On the one hand, the residual

water is low and the drainage performance rank is excellent; on the other hand, the gradation of drainage layer can accommodate the hydraulic conductivity to satisfy the strength of the drainage layer.

In summary, the saturated flow-based model, without considering the effect of vadose zone, failed to predict the behaviour of the drainage system in terms of both water seepage and drainage time (Dan et al., 2013; Xin et al., 2016). This highlights a major shortcoming of the current saturated flow-based model for designing subsurface drainage systems of a highway (Dan et al., 2012a; Dan et al., 2013; Skaggs, Youssef, & Chescheir, 2012). Certainly, there are some shortcomings in this paper which should be pointed out. For instance, the proposed model neglected the vertical flow in the drainage layer, and the seepage face was assumed to be zero in the drainage process for simplifying the solution derivation. The water retention curve was used as the Gardner function which is relatively simple. Moreover, it is inconvenient to evaluate the parameter (α_G and β_G) in the Gardner function of the drainage material, both of which should be obtained by experiment. To date, some researches were presented (Arya, Bowman, Thapa, & Cassel, 2008; Arya, Leij, van Genuchten, & Shouse, 1999) as alternative approaches to solve these problems. Nevertheless, in comparison, the present analytical model, which is simple and easy to use, has made a significant improvement in terms of process understanding and applications to engineering designs.

Disclosure statement

No potential conflict of interest was reported by the authors.

Funding

This research was supported by the National Natural Science Foundation of China (grant no. 51308554), the Guizhou Transportation Science and Technology Foundation (grant no. 2013-121-013) and the Hunan Transportation Science and Technology Foundation (grant no. 201622) to the first author. The Initial Funding of Specially-appointed Professorship (grant no. 502045001) is also appreciated.

ORCID

Han-Cheng Dan  <http://orcid.org/0000-0002-2817-3005>

Xiang Liu  <http://orcid.org/0000-0002-4933-9756>

References

- AASHTO. (1993). Guide for design of pavement structures, American Association of State and Highway Transportation Officials, Washington, DC.
- Al-Qadi, I. L., Lahouar, S., Louizi, A., Elseifi, M. A., & Wilkes, J. A. (2004). Effective approach to improve pavement drainage layers. *Journal of Transportation Engineering*, 130(5), 658–664.
- Arya, L. M., Bowman, D. C., Thapa, B. B., & Cassel, D. K. (2008). Scaling soil water characteristics of golf course and athletic field sands from particle-size distribution. *Soil Science Society of America Journal*, 72(1), 25–32.
- Arya, L. M., Leij, F. J., van Genuchten, M. T., & Shouse, P. J. (1999). Scaling parameter to predict the soil water characteristic from particle-size distribution data. *Soil Science Society of America Journal*, 63(3): 510–519.
- Averjanov, S. F. (1950). About permeability of subsurface soils in case of incomplete saturation. *Engineering Collection*, 7, 19–21.
- Bakker, M. (2004). Transient analytic elements for periodic Dupuit-Forchheimer flow. *Advances in Water Resources*, 27(1), 3–12.

- Barber, E. S., & Sawyer, C. L. (1952). Highway subdrainage. Proceedings, Highway Research Board, 643–666.
- Bear, J., & Verruijt, A. (1987). *Modeling groundwater flow and pollution*. Dordrecht: D. Reidel Publishing.
- Casagrande, A., & Shannon, W. L. (1952). Base course drainage for airport pavements. *Proceedings of the American society of civil engineers*, 77: 792–814.
- Cedergren, H. R. (1974). *Drainage of highway and airfield pavements*. New York, NY: Wiley.
- Dan, H.-C., He, L.-H., & Xu, B. (2016). Experimental investigation on non-Darcian flow in unbound graded aggregate material of highway pavement. *Transport in Porous Media*, 112, 189–206.
- Dan, H.-C., He, L.-H., Zhao, L. H., & Chen, J. Q. (2015). Coupled hydro-mechanical response of saturated asphalt pavement under moving traffic load. *International Journal of Pavement Engineering*, 16(2), 125–143.
- Dan, H.-C., Xin, P., Li, L., & Li, L. (2013). Improved Boussinesq equation-based model for transient flow in a drainage layer of highway: Capillary correction. *Journal of Irrigation and Drainage Engineering*, 139(12), 1018–1027.
- Dan, H.-C., Xin, P., Li, L., Li, L., & Lockington, D. (2012a). Boussinesq equation-based model for flow in the drainage layer of highway with capillarity correction. *Journal of Irrigation and Drainage Engineering*, 138(4), 336–348.
- Dan, H.-C., Xin, P., Li, L., Li, L., & Lockington, D. (2012b). Capillary effect on flow in the drainage layer of highway pavement. *Canadian Journal of Civil Engineering*, 39(6), 654–666.
- Dawson, A. (2008). *Water in road structure*. Berlin: Springer.
- FHWA. (1992). Demonstration project no. 87: Drainage pavement system participant notebook. Publication No. HWA-SA-92-008, Washington, DC.
- Gardner, W. R. (1958). Some steady-state solutions of the unsaturated moisture flow equation with application to evaporation from a water table. *Soil Science*, 85(4), 228–232.
- Gardner, W. R. (1962). Approximate solution of a non-steady state drainage problem. *Soil Science Society of American Journal*, 26(2), 129–132.
- Gureghian, A. B. (1978). Solutions of Boussinesq's equation for seepage flow. *Water Resources Research*, 14(2), 231–236.
- Hogarth, W. L., Parlange, J. Y., Parlange, M. B., & Lockington, D. (1999). Approximate analytical solution of the Boussinesq equation with numerical validation. *Water Resources Research*, 35(10), 3193–3197.
- Kong, J., Shen, C. J., Luo, Z. Y., Hua, G. F., & Zhao, H. J. (2016). Improvement of the hillslope-storage Boussinesq model by considering lateral flow in the unsaturated zone. *Water Resources Research*, 52(4), 2965–2984.
- Li, L., Lockington, D. A., Parlange, M. B., Stagnitti, F., Jeng, D. S., Selker, J. S., . . . Parlange, J. Y. (2005). Similarity solution of axisymmetric flow in porous media. *Advances in Water Resources*, 28(10), 1076–1082.
- Mallela, J., Titus-Glover, L., & Darter, M. I. (2000). Considerations for providing subsurface drainage in jointed concrete pavements. Transportation research record, 1709, Transportation Research Board, Washington, DC, 1–10.
- Ministry of Transport of the People's Republic of China (MOTPRC). (2006). *Specifications for design of highway asphalt pavement*. Washington, DC: China Communications Press.
- Ministry of Transport of the People's Republic of China (MOTPRC). (2012). *Specifications for drainage design of highway*. Washington, DC: China Communications Press.
- Moulton, L. K. (1979). *Groundwater, seepage, and drainage: A textbook on groundwater and seepage theory and its application*. Washington, DC: Federal Highway Administration (FHWA).
- Mualem, Y. (1978). Hydraulic conductivity of unsaturated porous media: Generalized macroscopic approach. *Water Resources Research*, 14(2), 325–334.
- Rabab'an, S. R. (2007). *Integrated assessment of free draining base and subbase materials under flexible pavement (PhD thesis)*. The University of Akron, Akron, OH.
- Richards, L. A. (1931). Capillary conduction of liquids through porous mediums. *Journal of Applied Physics*, 1(5), 318–333.
- Serrano, S. E., & Workman, S. R. (1998). Modeling transient stream/aquifer interaction with the non-linear boussinesq equation and its analytical solution. *Journal of Hydrology*, 206(3–4), 245–255.
- Skaggs, R. W., Youssef, M. A., & Chescheir, G. M. (2012). DRAINMOD: Model use, calibration, and validation. *Transactions of the ASABE*, 55, 1509–1522.
- Smith, R. E. (2002). *Infiltration theory for hydrologic applications*. Washington, DC: American Geophysical Union.

- Srivastava, R., & Yeh, T. C. J. (1991). Analytical solutions for one-dimensional, transient infiltration toward the water-table in homogeneous and layered soils. *Water Resources Research*, 27(5), 753–762.
- Verhoest, N. E. C., & Troch, P. A. (2000). Some analytical solutions of the linearized boussinesq equation with recharge for a sloping aquifer. *Water Resources Research*, 36(3), 793–800.
- Voss, C. I., & Provost, A. M. (2008). *A model for saturated-unsaturated, variable-density ground-water flow with solute or energy transport* (Water-Resources Investigations Report, 02-4231). Reston, VA: Geological Survey.
- Xin, P., Dan, H.-C., Zhou, T., Lu, C., Kong, J., & Li, L. (2016). An analytical solution for predicting the transient seepage from a subsurface drainage system. *Advances in Water Resources*, 91(5), 1–10.
- Youngs, E. G., & Rushton, K. R. (2009). Dupuit-forchheimer analyses of steady-state water-table heights due to accretion in drained lands overlying undulating sloping impermeable beds. *Journal of Irrigation and Drainage Engineering*, 135(4), 467–473.